Phosphorus-doped protonic conductors based on BaLa$_n$In$_n$O$_{3n+1}$ (n = 1, 2): applying oxyanion doping strategy to the layered perovskite structures

Natalia Tarasova *[iD], Anzhelika Galisheva [iD]

Institute of High Temperature Electrochemistry, the Ural Branch of the Russian Academy of Sciences, Ekaterinburg 620990, Russia.

* Corresponding author: Natalia.Tarasova@urfu.ru

This paper belongs to a Regular Issue.

Abstract

The creation of highly efficient and eco-friendly energy sources such as hydrogen energy systems is one of main vectors for the sustainable development of human society. Proton-conducting ceramic materials can be applied as one of the main components of such hydrogen-fueled electrochemical devices, including protonic ceramic fuel cells. The oxyanion doping strategy is a promising approach for improving transport properties of proton-conducting complex oxides. In this paper, this strategy was applied to proton-conducting layered perovskites for the first time. The phosphorus-doped protonic conductors based on BaLa$_n$In$_n$O$_{3n+1}$ (n = 1, 2) were obtained, and their electrical conductivity was thoroughly investigated. It was found that the phosphorous doping leads to an increase in the electrical conductivity values by ~0.7 orders of magnitude.

Key findings

● The oxyanion doping strategy is a promising method for improving transport properties of proton-conducting layered perovskites.

● The phosphorous-doping leads to a considerable increase of electrical conductivity of the BaLaIn$_{0.9}$P$_{0.1}$O$_{4.1}$ and BaLa$_2$In$_{1.9}$P$_{0.1}$O$_{7.1}$ compared to the P-free materials.

1. Introduction

The creation of high-efficiency and eco-friendly energy source is one of main objectives for the sustainable global development of human society [1–8]. Hydrogen energy belongs to the renewable energy industry and includes the systems for storage, transport and using of hydrogen for power generation [9–12]. Proton-conducting ceramic materials can be applied as the one of main component of such hydrogen-based electrochemical devices for various purposes, including electricity generation in protonic ceramic fuel cells, PCFCs [13–25]. The most studied protonic conductors have perovskite or perovskite-related structures [26–30]. Doping of cationic sublattices is a common way for improving their transport properties. However, the anion [31–35] and oxyanion [36, 37] doping methods can increase proton conductivity in the complex oxides as well. The oxyanion doping strategy is based on the displacement of the [BO$_6$] octahedra to the [B'O$_4$] tetrahedra such as phosphate, sulphate and silicate (Figure 1). Slater

et al. proved the validity of this strategy for the proton-conducting materials, studying barium indate, Ba$_2$In$_2$O$_5$, as an example [36]. This confirms that substitution [PO$_4$] → [InO$_6$] is fundamentally possible, and the proton conductivity in such compositions can be improved by phosphorus doping.

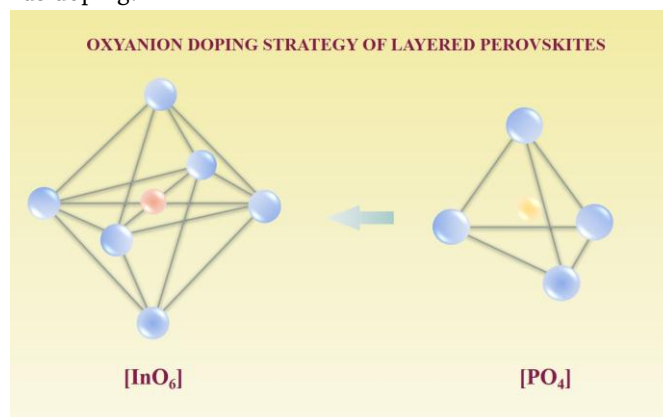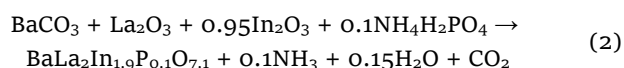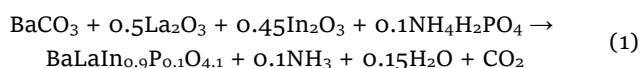**Figure 1** The scheme of oxyanion doping strategy of layered perovskites.

Barium lanthanum indates, $BaLaInO_4$ and $BaLa_2In_2O_7$, have a layered perovskite structure and can be written using a general formula, $BaLa_nIn_nO_{3n+1}$ (n = 1, 2). They belong to the newly opened class of proton-conducting solid oxide materials [38–49]. It was proved that they are nearly pure (~95–98 %) protonic conductors under wet air below 350–400 °C [50]. Different ways of cationic (iso- and heterovalent) doping lead to increasing the protonic conductivity up to ~1.5 orders of magnitude (from $2 \cdot 10^{-7}$ S cm^{-1} for $BaLaInO_4$ to $8 \cdot 10^{-6}$ S cm^{-1} for $Ba_{1.1}LaInO_{3.95}$ at 400 °C) [51–56]. Based on this fact, the other doping strategies, such as oxyanion (phosphorus) doping, can be applied to these materials. The reason of this materials search is necessity to create high-conductive proton conductors with the layered perovskite structure because the promising cathode materials based on nickelates lanthanides [57–60] belong to the layered perovskites as well.

In the present study, the oxyanion doping strategy was applied to the proton-conducting layered perovskites for the first time. The phosphorus-doped protonic conductors based on $BaLa_nIn_nO_{3n+1}$ (n = 1, 2) were obtained, and electrical conductivity of ceramic samples was investigated.

2. Experimental

The complex oxides of $BaLaIn_{0.9}P_{0.1}O_{4.1}$ and $BaLa_2In_{1.9}P_{0.1}O_{7.1}$ were obtained by a solid state method. Firstly, high-purity starting powder materials were dried and the stoichiometric amounts of the reagents were weighed on a Sartorius analytical balances (Goettingen, Germany). The chemical reactions can be presented in as:

$$BaCO_3 + 0.5La_2O_3 + 0.45In_2O_3 + 0.1NH_4H_2PO_4 \rightarrow$$
$$BaLaIn_{0.9}P_{0.1}O_{4.1} + 0.1NH_3 + 0.15H_2O + CO_2 \tag{1}$$

$$BaCO_3 + La_2O_3 + 0.95In_2O_3 + 0.1NH_4H_2PO_4 \rightarrow$$
$$BaLa_2In_{1.9}P_{0.1}O_{7.1} + 0.1NH_3 + 0.15H_2O + CO_2 \tag{2}$$

Further, the milling of all reagents in an agate mortar followed by calcination of the obtained mixtures was made. The calcination was performed in a temperature range from 800 to 1300 °C with a step of 100 °C and 24 h of time treatments.

The X-ray diffraction (XRD) studies were performed by a Bruker Advance D8 diffractometer (Rheinstetten, Germany) with a Cu Kα radiation with a step of 0.01° and at a scanning rate of 0.5° min^{-1}. The morphology and chemical composition of the samples were studied using a Phenom ProX Desktop scanning electron microscope (Waltham, MA, USA) (SEM) integrated with an energy-dispersive X-ray diffraction (EDS) detector.

For the investigations of the electrical properties, the pressed cylindrical pellets (1300 °C, 24 h, dry air) were obtained. The samples had a relative density of ~90%

(density of the sintered samples was determined by the Archimedes method). The AC conductivity measurements were performed by a Z-1000P (Elins, RF) impedance spectrometer within a frequency range of $1–10^6$ Hz. Electrical measurements were performed using Pt paste electrodes (sintering at 1000 °C for 2 h). The temperature dependencies of electrical conductivity were obtained in a temperature range 200–1000 °C (step 10–20 °C, 1 °C min^{-1} cooling rate). These investigations were performed under "dry" and "wet" air atmospheres. The dry air was produced by circulating the gas through P_2O_5 (pH$_2$O = $3.5 \cdot 10^{-5}$ atm). The wet air was obtained by bubbling the gas at room temperature first through distilled water and then through a saturated solution of KBr (pH$_2$O = $2 \cdot 10^{-2}$ atm). The humidity of the gas was controlled by a Honeywell HIH-3610 H$_2$O-sensor (Freeport, USA).

3. Results and discussions

The XRD analysis of the powder samples $BaLaIn_{0.9}P_{0.1}O_{4.1}$ and $BaLa_2In_{1.9}P_{0.1}O_{7.1}$ confirmed the single phase for both compositions. The XRD-patterns for the compositions of $BaLaIn_{0.9}P_{0.1}O_{4.1}$ and $BaLa_2In_{1.9}P_{0.1}O_{7.1}$ are presented in the Figure 2 and 3 correspondingly.

Phosphorous-doped $BaLaIn_{0.9}P_{0.1}O_{4.1}$ and $BaLa_2In_{1.9}P_{0.1}O_{7.1}$ samples are isostructural to theirs matrix compositions, $BaLaInO_4$ and $BaLa_2In_2O_7$, correspondingly. The monolayer $BaLaIn_{0.9}P_{0.1}O_{4.1}$ composition belongs to the *Pbca* space group (orthorhombic symmetry), and the two-layered composition of $BaLa_2In_{1.9}P_{0.1}O_{7.1}$ crystallizes in the $P4_2/mnm$ space group (tetragonal symmetry). The values of lattice parameters and unit cell volume are presented in Table 1.
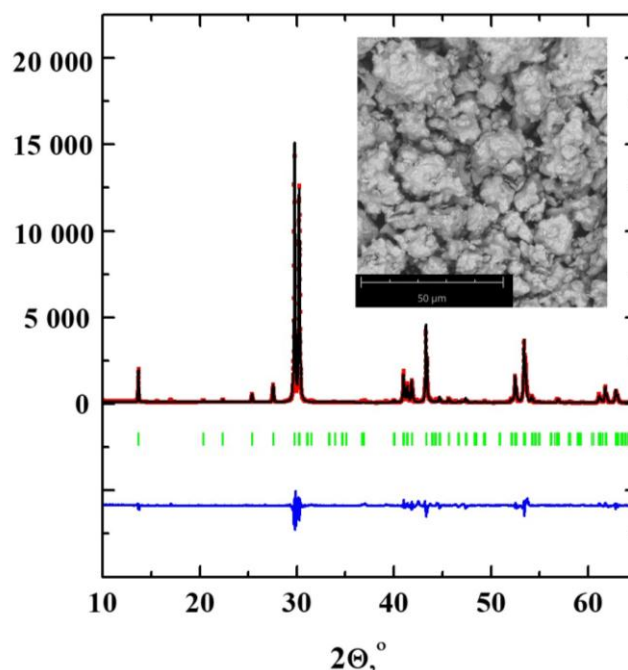

Figure 2 The XRD-results for $BaLaIn_{0.9}P_{0.1}O_{4.1}$ composition. The SEM-image is presented in the inset.
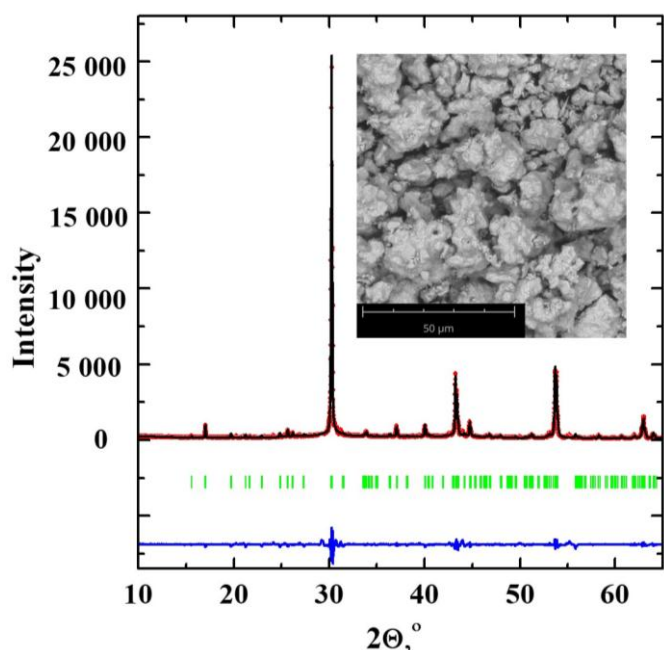
Figure 3 The XRD-results for $BaLa_2In_{1.9}P_{0.1}O_{7.1}$ composition. The SEM-image is presented in the inset.

Table 1 The lattice parameters and unit cell volume of investigated compositions.

Composition	a, Å	b, Å	c, Å	V, Å³
$BaLaInO_4$ [50]	12.932	5.906	5.894	450.19
$BaLaIn_{0.9}P_{0.1}O_{4.1}$	12.803	5.939	5.906	449.04
$BaLa_2In_2O_7$ [50]	5.891	5.891	20.469	710.520
$BaLa_2In_{1.9}P_{0.1}O_{7.1}$	5.909	5.909	20.868	728.605

As can be seen, phosphorous-doping leads to a change in these characteristics for both doped compositions compared with undoped. The oxyanion doping for the monolayer composition of $BaLaInO_4$ leads to a decrease in the a parameter and to an increase in the b and c parameters. The applying of this doping strategy to the two-layered compositions of $BaLa_2In_2O_7$ leads to an increase of all (a, b and c) lattice parameters. As it is known [61], the ionic radius of phosphorous is smaller than ionic radius of indium ($r(P^{5+})$ = 0.38 Å, $r(In^{3+})$ = 0.8 Å). However, the displacement of $[InO_6]$ octahedra to the $[PO_4]$ tetrahedra should inevitably lead to the appearance of local distortions and to a redistribution of bond lengths in the crystal structure. The microphotography (SEM-image) of the $BaLa_2In_{1.9}P_{0.1}O_{7.1}$ powder sample is presented in the inset of Figure 3. This composition consists of grains ~5 μm, forming agglomerates of ~15–30 μm.

The electrical conductivity was measured by the impedance spectroscopy method. The Nyquist-plots for $BaLaIn_{0.9}P_{0.1}O_{4.1}$ composition obtained under dry air are presented in the Figure 4a, b. The fitting of the spectra was made using ZView software, and the obtained results are presented in the Table 2. According to the fitting of the spectra (red line) with using the equivalent circuit presented in the Figure 4c, three different electrochemical processes can be defined. As it was shown earlier [51], the Nyquist-plots for undoped $BaLaInO_4$ composition were

represented by one visible semicircle with a capacitance of around 10^{-11} F. For the calculation of electrical conductivity, the bulk resistance values (R1) were used and discussed below. It can be noted, that due to a small depression of the semicircles, the constant phase element (CPE) was used during the analysis of Nyquist plots.

The results of the electrical conductivity investigations are presented in the Figure 5. As can be seen, phosphorous-doping leads to an increase in the conductivity values for both monolayer ($BaLaInO_4$) and two-layered ($BaLa_2In_2O_7$) compositions and. The conductivity growth is about 0.7 orders of magnitude for both compositions. We can assume that such increasing electrical conductivity is due to two factors. Firstly, an increase in the lattice parameters for the layered perovskites of $BaLa_nIn_nO_{3n+1}$ results in a higher conductivity due to facilitating ionic transport [50]. Secondly, the phosphorous-doping can be considered as a donor doping ($P^{5+} \rightarrow In^{3+}$) that causes the appearance of interstitial ("additional") oxygen in the structure. It is obvious that an increase in the concentration of charge carriers (oxygen ions) should lead to the corresponding increase in the conductivity as well.

The change in atmospheric humidity also affects the electrical conductivity values (Figure 5). The air humudification leads to an increase in the conductivity values at low temperatures (450 °C).
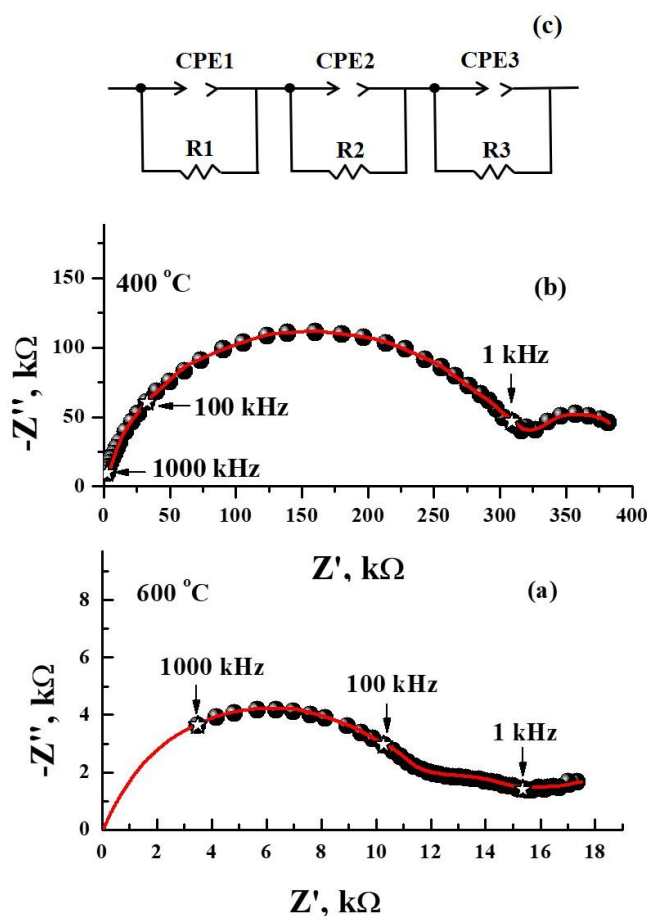

Figure 4 The Nyquist-plots obtained at the different temperatures under dry air for the composition $BaLaIn_{0.9}P_{0.1}O_{4.1}$: 600 °C (a), 500 °C (b), and the equivalent circuit of fitting (red line) (c).

Table 2 Results of Nyquist-plots fitting, where CPE is the constant phase element (F) and the R is the resistance (kΩ).

Element	Value (600 °C)	Value (500 °C)
CPE1	$2.1 \cdot 10^{-12}$	$3.6 \cdot 10^{-12}$
R_1	11	280
CPE2	$4.5 \cdot 10^{-10}$	$4.8 \cdot 10^{-10}$
R_2	4.5	40
CPE3	$3.4 \cdot 10^{-7}$	$5.1 \cdot 10^{-7}$
R_3	2	70
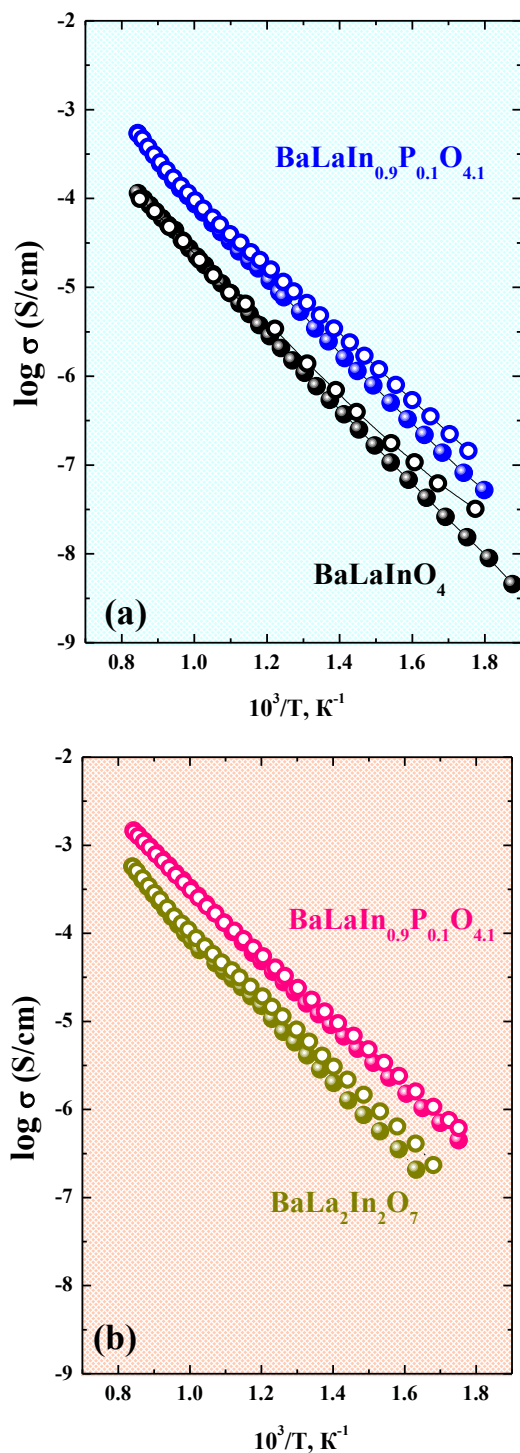
Figure 5 The temperatures dependencies of conductivity for the compositions $BaLaIn_{0.9}P_{0.1}O_{4.1}$ (a) and $BaLa_2In_{1.9}P_{0.1}O_{7.1}$ (b) under dry (filled symbols) and wet (open symbols) air.

Because layered perovskites $BaLaInO_4$ and $BaLa_2In_2O_7$ are capable for the dissociative absorption of water from the gas phase [50], the reason of better conductivity is the appearance of proton contribution of conductivity. It can be concluded that the oxyanion doping strategy can be applied for layered perovskites for improving their transport properties.

4. Conclusions

In this paper, the oxyanion doping strategy was purposefully applied to the proton-conducting layered perovskites for the first time. The phosphorus-doped protonic conductors based on $BaLa_nIn_nO_{3n+1}$ (n = 1, 2) were obtained, and their electrical properties were investigated. The $BaLaIn_{0.9}P_{0.1}O_{4.1}$ and $BaLa_2In_{1.9}P_{0.1}O_{7.1}$ oxides were obtained for the first time. It was found that the phosphorous-doping leads to an increase in the electrical conductivity values by ~0.7 orders of magnitude. The oxyanion doping strategy is a promising method for improving transport properties of proton-conducting layered perovskites.

Supplementary materials

No supplementary materials are available.

Funding

Acknowledgments

Author contributions

Conceptualization: N.T.
Data curation: A.G., N.T.
Methodology: N.T.
Validation: A.G., N.T.
Visualization: A.G., N.T.
Writing – original draft: N.T.
Writing – review & editing: N.T.

Conflict of interest

The authors declare no conflict of interest.

Additional information

Author IDs:
    Natalia Tarasova, Scopus ID 37047923700;
    Anzhelika Galisheva, Scopus ID 57195274932.

Website:

Institute of High Temperature Electrochemistry UB RAS, http://www.ihte.uran.ru/

References

1. Panwar NL, Kaishik SC, Kothari S. Winkler T, Sass FA, Duda GN, Schmidt-Bleek K. Role of renewable energy sources in environmental protection: A review. Renew Sustain Energy Rev. 2011;15(3):1513–1524. doi:10.1016/j.rser.2010.11.037

2. Chu S, Majumdar A. Opportunities and challenges for a sustainable energy future. Nature. 2012;488:294–303. doi:10.1038/nature11475

3. Dincer I, Rosen MA. Sustainability aspects of hydrogen and fuel cell systems. Int J Sustain Energy Dev. 2011;15(2):137–146. doi:10.1016/j.esd.2011.03.006

4. Branco H, Castro R, Lopes AS. Battery energy storage systems as a way to integrate renewable energy in small isolated power systems. Int J Sustain Energy Dev. 2018;43:90–99. doi:10.1016/j.esd.2018.01.003

5. Malerba D. Poverty-energy-emissions pathways: Recent trends and future sustainable development goals. Int J Sustain Energy Dev. 2019;49:109–124. doi:10.1016/j.esd.2019.02.001

6. Buonomano A, Barone G, Forzano C. Advanced energy technologies, methods, and policies to support the sustainable development of energy, water and environment systems. Energy Rep. 2022;8:4844–4853. doi:10.1016/j.egyr.2022.03.171

7. Olabi AG, Abdelkareem MA. Renewable energy and climate change. Renew Sustain Energy Rev. 2022;158:112111. doi:10.1016/j.rser.2022.112111

8. Østergaard PA, Duic N, Noorollahi Y, Mikulcic H, Kalogirou S. Sustainable development using renewable energy technology. Renew Energy. 2020;146:2430–2437. doi:10.1016/j.renene.2019.08.094

9. International Energy Agency. The Future of Hydrogen: Seizing today's opportunities. OECD. 2019. doi:10.1787/1e0514c4-en

10. Abdalla AM, Hossain S, Nisfindy OB, Azad AT, Dawood M, Azad AK. Hydrogen production, storage, transportation and key challenges with applications: A review. Energy Convers Manag. 2018;165:602–627. doi:10.1016/j.enconman.2018.03.088

11. Dawood F, Anda M, Shafiullah GM. Hydrogen production for energy: An overview. Int J Hydrog Energy. 2020;45(7):3847–3869. doi:10.1016/j.ijhydene.2019.12.059

12. Arsad AZ, Hannan MA, Al-Shetwi AQ, Mansur M, Muttaqi KM, Dong ZY, Blaabjerg F. Hydrogen energy storage integrated hybrid renewable energy systems: A review analysis for future research directions. Int J Hydrog Energy. 2022;47(39):17285–17312. doi:10.1016/j.ijhydene.2022.03.208

13. Hossain S, Abdalla AM, Jamain SNB, Zaini JH, Azad AK. A review on proton conducting electrolytes for clean energy and intermediate temperature-solid oxide fuel cells. Renew Sustain Energy Rev. 2017;79:750–764. doi:10.1016/j.rser.2017.05.147

14. Kim J, Sengodan S, Kim S, Kwon O, Bu Y, Kim G. Proton conducting oxides: A review of materials and applications for renewable energy conversion and storage. Renew Sustain Energy Rev. 2019;109:606–618. doi:10.1016/j.rser.2019.04.042

15. Zhang W, Hu YH. Progress in proton-conducting oxides as electrolytes for low-temperature solid oxide fuel cells: From materials to devices. Energy Sci Eng. 2021;9(7):984–1011. doi:10.1002/ese3.886

16. Meng Y, Gao J, Zhao Z, Amoroso J, Tong J, Brinkman KS. Review: recent progress in low-temperature proton-conducting ceramics. J Mater Sci. 2019;54:9291–9312. doi:10.1007/s10853-019-03559-9

17. Medvedev D. Trends in research and development of protonic ceramic electrolysis cells. Int J Hydrog Energy. 2019;44(49):26711–26740. doi:10.1016/j.ijhydene.2019.08.130

18. Medvedev DA. Current drawbacks of proton-conducting ceramic materials: How to overcome them for real electrochemical purposes. Curr Opin Green Sustain Chem. 2021;32:100549. doi:10.1016/j.cogsc.2021.100549

19. Zvonareva I, Fu X-Z, Medvedev D, Zhao Z. Electrochemistry and energy conversion features of protonic ceramic cells with mixed ionic-electronic electrolytes. Energy Environ Sci. 2022;15:439–465. doi:10.1039/D1EE03109K

20. Shim JH. Ceramics breakthrough. Nature Energy. 2018;3:168–169. doi:10.1038/s41560-018-0110-7

21. Bello IT, Zhai S, He Q, Cheng C, Dai Y, Chen B, Zhang Y, Ni M. Materials development and prospective for protonic ceramic fuel cells. Int J Energy Res. 2021;46(3):2212–2240. doi:10.1002/er.7371

22. Irvine J et al. Roadmap on inorganic perovskites for energy applications. J Phys Energy. 2021;3:031502. doi:10.1088/2515-7655/abff18

23. Chiara A, Giannici F, Pipitone C, Longo A, Aliotta M, Gambino M, Martorana A. Solid-Solid Interfaces in Protonic Ceramic Devices: A Critical Review. ACS Appl Mater Interfaces. 2020;12:55537–55553. doi:10.1021/acsami.0c13092

24. Cao J, Ji Y, Shao Z. New Insights into the Proton-Conducting Solid Oxide Fuel Cells. J Chin Ceram Soc. 2021;49:83–92. doi:10.14062/j.issn.0454-5648.20200390

25. Bello IT, Zhai S, Zhao S, Li Z, Yu N, Ni M. Scientometric review of proton-conducting solid oxide fuel cells. Int J Hydrog Energy. 2021;46(75):37406–37428. doi:10.1016/j.ijhydene.2021.09.061

26. Iwahara H, Esaka T, Uchida H, Maeda N. Proton conduction in sintered oxides and its application to steam electrolysis for hydrogen production. Solid State Ion. 1981;3–4:359–363. doi:10.1016/0167-2738(81)90113-2

27. Iwahara H, Uchida H, Maeda N. High temperature fuel and steam electrolysis cells using proton conductive solid electrolytes. J Power Sources. 1982;7(3):293–301. doi:10.1016/0378-7753(82)80018-9

28. Tarasova N, Colomban P, Animitsa I. The short-range structure and hydration process of fluorine-substituted double perovskites based on barium-calcium niobate $Ba_2CaNbO_{5.5}$. J Phys Chem Solids. 2018;118:32–39. doi:10.1016/j.jpcs.2018.02.049

29. Fop S, McCombie KS, Wildman EJ, Skakle MS, Irvine JTS, Connor PA, Savaniu C, Ritter C, Mclaughlin AC. High oxide ion and proton conductivity in a disordered hexagonal perovskite. Nature Mater. 2020;19:752–757. doi:10.1038/s41563-020-0629-4

30. Yashima M, Tsujiguchi T, Sakuda Y, Yasui Y, Zhou Y, Fujii K, Torii S, Kamiyama T, Skinner SJ. High oxide-ion conductivity through the interstitial oxygen site in $Ba_7Nb_4MoO_{20}$-based hexagonal perovskite related oxides. Nature Comm. 2021;12:556. doi:10.1038/s41467-020-20859-w

31. Wang Y, Wang H, Liu T, Chen F, Xia C. Improving the chemical stability of $BaCe_{0.8}Sm_{0.2}O_{3-\delta}$ electrolyte by Cl doping for proton-conducting solid oxide fuel cell. Electrochem Comm. 2013;28:87–90. doi:10.1016/j.elecom.2012.12.012

32. Zhou H, Dai L, Jia L, Zhu J, Li Y, Wang L. Effect of fluorine, chlorine and bromine doping on the properties of gadolinium doped barium cerate electrolytes. Int J Hydrog Energy. 2015;40(29):8980–8988. doi:10.1016/j.ijhydene.2015.05.040

33. Tarasova N, Animitsa I. The influence of anionic heterovalent doping on transport properties and chemical stability of F-, Cl-doped brownmillerite $Ba_2In_2O_5$. J Alloys Compd. 2018;739:353–359. doi:10.1016/j.jallcom.2017.12.317

34. Ushakov AE, Merkulov OV, Markov AA, Patrakeev MV, Leonidov IA. Ceramic and transport properties of halogen-substituted strontium ferrite. Ceram Int. 2018;44(10):11301–11306. doi:10.1016/j.ceramint.2018.03.177

35. Liu J, Jin Z, Miao L, Ding J, Tang H, Gong Z, Peng R, Liu W. A novel anions and cations co-doped strategy for developing high-performance cobalt-free cathode for intermediate-temperature proton-conducting solid oxide fuel cells. Int J Hydrog Energy. 2019;44(21):11079–11087. doi:10.1016/j.ijhydene.2019.03.001

36. Shin JF, Orera A, Apperley DC, Slater PR. Oxyanion doping strategies to enhance the ionic conductivity in $Ba_2In_2O_5$. J Mater Chem. 2011;21(3):874–879. doi:10.1039/c0jm01978j

37. Hancock CA, Porras-Vazquez JM, Keenan PJ, Slater PR. Oxyanions in perovskites: from superconductors to solid oxide fuel cells. Dalton Trans. 2015;44(23):10559. doi:10.1039/c4dt03036b

38. Tarasova N, Animitsa I. $A^{II}LnInO_4$ with Ruddlesden-Popper structure for electrochemical applications: relationship between ion (oxygen-ion, proton) conductivity, water uptake and structural changes. Materials. 2022;15(1):114. doi:10.3390/ma15010114

39. Fujii K, Shiraiwa M, Esaki Y, Yashima M, Hoshikawa A, Ishigaki T, Hester JR. New Perovskite-Related Structure Family of Oxide-Ion Conducting Materials $NdBaInO_4$. Chem Mater. 2014;26(8):2488–2491. doi:10.1021/cm500776x

40. Fujii K, Shiraiwa M, Esaki Y, Yashima M, Kim SJ, Lee S. Improved oxide-ion conductivity of $NdBaInO_4$ by Sr doping. J Mater Chem A. 2015;3(22):11985–11990. doi:10.1039/c5ta01336d

41. Ishihara T, Yan Y, Sakai T, Ida S. Oxide ion conductivity in doped $NdBaInO_4$. Solid State Ion. 2016;288:262–265. doi:10.1016/j.ssi.2016.01.011

42. Yang X, Liu S, Lu F, Xu J, Kuang X. Acceptor Doping and Oxygen Vacancy Migration in Layered Perovskite $NdBaInO_4$-Based Mixed Conductors. J Phys Chem C, 2016;12:6416–6426. doi:10.1021/acs.jpcc.6b00700

43. Fujii K, Yashima M. Discovery and development of $BaNdInO_4$ - A brief review. J Ceram Soc Japan. 2018;126(10):852–859. doi:10.2109/jcersj2.18110

44. Zhou Y, Shiraiwa M, Nagao M, Fujii K, Tanaka I, Yashima M, Baque L, Basbus JF, Mogni LV, Skinner SJ. Protonic Conduction in the $BaNdInO_4$ Structure Achieved by Acceptor Doping. Chem Mater. 2021;33(6):2139–2146. doi:10.1021/acs.chemmater.0c04828

45. Kato S, Ogasawara M, Sugai M, Nakata S. Synthesis and oxide ion conductivity of new layered perovskite $La_{1-x}Sr_{1+x}InO_{4-d}$. Solid State Ion. 2002;149(1–2):53–57. doi:10.1016/S0167-2738(02)00138-8.

46. Troncoso L, Alonso JA, Aguadero A. Low activation energies for interstitial oxygen conduction in the layered perovskites $La_{1+x}Sr_{1-x}InO_{4+d}$. J Mater Chem A. 2015;3(34):17797–17803. doi:10.1039/c5ta03185k

47. Troncoso L, Alonso JA, Fernández-Díaz MT, Aguadero A. Introduction of interstitial oxygen atoms in the layered perovskite $LaSrIn_{1-x}B_xO_{4+\delta}$ system (B=Zr, Ti). Solid State Ionics. 2015;282:82–87. doi:10.1016/j.ssi.2015.09.014

48. Troncoso L, Mariño C, Arce MD, Alonso JA. Dual oxygen defects in layered $La_{1.2}Sr_{0.8-x}Ba_xInO_{4+d}$ (x = 0.2, 0.3) oxide-ion conductors: a neutron diffraction study. Mater. 2019;12(10):1624. doi:10.3390/ma12101624

49. Troncoso L, Arce MD, Fernández-Díaz MT, Mogni LV, Alonso JA. Water insertion and combined interstitial-vacancy oxygen conduction in the layered perovskites $La_{1.2}Sr_{0.8-x}Ba_xInO_{4+d}$. New J Chem. 2019;43(15):6087–6094. doi:10.1039/C8NJ05320K

50. Tarasova N, Galisheva A, Animitsa I, Korona D, Kreimesh H, Fedorova I. Protonic Transport in Layered Perovskites $BaLa_nIn_nO_{3n+1}$ (n = 1, 2) with Ruddlesden-Popper Structure. Appl Sci. 2022;12(8):4082. doi:10.3390/app12084082

51. Tarasova N, Animitsa I, Galisheva A. Electrical properties of new protonic conductors $Ba_{1+x}La_{1-x}InO_{4-0.5x}$ with Ruddlesden-Popper structure. J Solid State Electrochem. 2020;24:1497–1508. doi:10.1007/s10008-020-04630-1

52. Tarasova N, Galisheva A, Animitsa I. Improvement of oxygen-ionic and protonic conductivity of $BaLaInO_4$ through Ti doping. Ionics. 2020;26:5075–5088. doi:10.1007/s11581-020-03659-6

53. Tarasova N, Galisheva A, Animitsa I. Ba^{2+}/Ti^{4+}- co-doped layered perovskite $BaLaInO_4$: the structure and ionic (O^{2-}, H^+) conductivity. Int J Hydrog Energy. 2021;46(32):16868–16877. doi:10.1016/j.ijhydene.2021.02.044

54. Tarasova NA, Galisheva AO, Animitsa IE, Lebedeva EL. Oxygen-Ion and Proton Transport in Sc-Doped Layered Perovskite $BaLaInO_4$. Russ J Electrochem. 2021;57(10):1008–1014. doi:10.1134/S1023193521080127

55. Tarasova N, Galisheva A, Animitsa I, Anokhina I, Gilev P, Cheremisina P. Novel mid-temperature $Y^{3+} \rightarrow In^{3+}$ doped proton conductors based on the layered perovskite $BaLaInO_4$. Ceram Int. 2022;48(11):15677–15685. doi:10.1016/j.ceramint.2022.02.102

56. Tarasova N, Galisheva A, Animitsa I, Korona D, Davletbaev K. Novel proton-conducting layered perovskite based on $BaLaInO_4$ with two different cations in B-sublattice: Synthesis, hydration, ionic (O^{2+}, H^+) conductivity. Int J Hydrog Energy. 2022;47(44):18972–18982. doi:10.1016/j.ijhydene.2022.04.112

57. Tarutin A, Lyagaeva J, Medvedev D, Bi L, Yaremchenko A. Recent advances in layered $Ln_2NiO_{4+\delta}$ nickelates: fundamentals and prospects of their applications in protonic ceramic fuel and electrolysis cells. J Mater Chem A. 2021;9(1):154–195. doi:10.1039/D0TA08132A

58. Tarutin A, Gorshkov Yu, Bainov A, Vdovin G, Vylkov A, Lyagaeva J, Medvedev D. Barium-doped nickelates $Nd_{2-x}Ba_xNiO_{4+\delta}$ as promising electrode materials for protonic ceramic electrochemical cells. Ceram Int. 2020;46(15):24355–24364. doi:10.1016/j.ceramint.2020.06.217

59. Tarutin A, Lyagaeva J, Farlenkov A, Plaksin S, Vdovin G, Demin A, Medvedev D. A Reversible protonic ceramic cell with symmetrically designed $Pr_2NiO_{4+\delta}$-based electrodes: fabrication and electrochemical features. Mater. 2019;12(1):118. doi:10.3390/ma12010118

60. Tarutin AP, Lyagaeva JG, Farlenkov AS, Vylkov AI, Medvedev DA. Cu-substituted $La_2NiO_{4+\delta}$ as oxygen electrodes for protonic ceramic electrochemical cells. Ceramic Int. 2019;45(13):16105–16112. doi:10.1016/j.ceramint.2019.05.127

61. Shannon RD, Revised effective ionic radii and systematic studies of interatomic distances in halides and chalcogenides. Acta Cryst. 1976;A32:751–767. doi:10.1107/S0567739476001551